Effect of Nano- to Millisecond Pulse on Dielectric Barrier Discharges

Article *in* IEEE Transactions on Plasma Science · June 2009

DOI: 10.1109/TPS.2009.2015321 · Source: IEEE Xplore

Effect of Nano- to Millisecond Pulse on Dielectric Barrier Discharges

XinPei Lu, *Senior Member, IEEE*, Qing Xiong, ZiLan Xiong, YuBin Xian, Fei Zhou, Jing Hu, WeiWei Gong, ChangLin Zhou, ZhiYuan Tang, ZhongHe Jiang, and Yuan Pan

***Abstract*—It has recently been demonstrated that pulsed direct-current (dc) voltages show better performance in generating diffuse plasmas under various conditions. However, it still remains unclear whether the pulsewidth or the rising and falling times of the voltage pulse play the essential role in the improvement of the performance of the dielectric barrier discharges (DBDs). In this paper, we focus on the effect of pulsewidth. Pulsed dc voltages with pulsewidth varying from 0.2 μs to about 1 ms are used to drive the DBDs. High-speed photographs show that diffuse Ar plasmas can be generated by pulsed dc voltages with pulsewidths covering the entire investigated range. It is found that the pulsewidths of the applied voltages affect the discharge current durations significantly when the pulsewidth is shorter than 600 ns or the break between the two consecutive pulses is shorter than 600 ns.**

***Index Terms*—Atmospheric-pressure plasma, dielectric barrier discharge (DBD), high-speed photograph, nonequilibrium plasma.**

I. Introduction

IN THE LAST decades, due to several emergent applications of atmospheric-pressure nonequilibrium plasmas, such as surface and material processing [1], [2], biological and chemical decontamination of media [3]–[9], absorption and reflection of electromagnetic radiation [10], [11], and synthesis of nanomaterials [12], [13], the generation of homogeneous plasmas (glowlike and Townsend-like modes) by using dielectric barrier discharges (DBDs) [14]–[21] has attracted significant attention. Traditionally, DBDs are driven by sine wave voltages with magnitudes in the kilovolt range and frequencies in the kilohertz range. Depending on the operating parameters, DBDs can generate either filamentary or diffuse plasmas. However, due to the instability of the plasma, the discharge can transit from a diffuse plasma to a filamentary plasma even when the operation conditions slightly change.

In order to generate stable diffuse plasmas, pulsed direct-current (dc) voltages have recently been introduced [22]–[25]. It has been demonstrated that nanosecond pulsed dc voltages are able to generate diffuse plasmas under various conditions [26]–[29]. Moreover, it has also been reported that the energy transfer efficiency can be improved by using submicrosecond voltage pulses, and the peak electron temperature of the plasma can reach as high as 8 eV [30], [31]. Meanwhile, most of the pulsed dc voltages used for driving the plasmas have much shorter rising and falling times than that of the kilohertz ac voltages. Therefore, it is not clear whether the pulsewidth t_w or the rising and falling times of the voltage pulse are essential for improving the performance of the DBDs. To improve the performance of pulsed DBD discharges, further investigations on the effects of the pulsewidth and the rising and falling times of the voltages are thus needed.

In this paper, to address this important issue, pulsed dc voltages with pulsewidths varying from 0.2 μs to 1 ms are used to drive the DBD. High-speed photographs show that diffuse plasmas can be generated by the pulsed dc voltages within the whole range of pulsewidths.

The rest of this paper is organized as follows. The experimental setup is described in Section II. Details of the experimental results, including the I–V characteristics of the discharge, high-speed photographs, and the emission spectra of the plasma are presented in Section III. Finally, the discussion of the experimental results is given in Section IV, and a brief conclusion of this paper is presented in Section V.

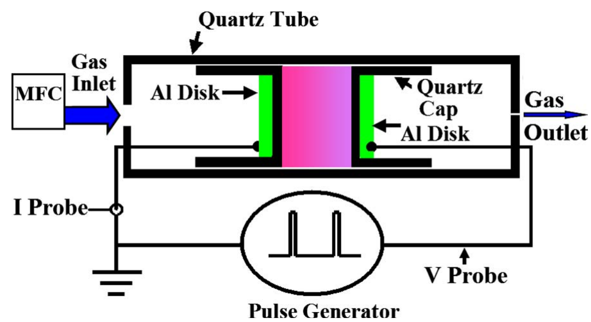

Fig. 1. Schematic of the experiment setup. Diameters of the quartz tube and the quartz caps are 24 and 22 mm, respectively. The gap distance is fixed at 6 mm.

II. Experiment Setup

The schematic of the experimental setup is shown in Fig. 1. Two aluminum disk electrodes are covered by two quartz caps. They are both inserted into a quartz tube. The inner diameter of the quartz tube is approximately 24 mm. The inner and the outer diameters of the two quartz caps are about 19 and 22 mm, respectively. The distance d between the two quartz caps can be varied from a few millimeters to about 10 cm. In this paper, d is fixed at 6 mm. To keep the gas contamination inside the quartz tube as low as possible, the right end of the quartz tube is

Manuscript received December 9, 2008; revised January 13, 2009 and February 7, 2009. First published April 7, 2009; current version published May 8, 2009. This work was supported in part by the National Natural Science Foundation under Grant 10875048 and in part by the Chang Jiang Scholars Program, Ministry of Education, People's Republic of China.

The authors are with the Nuclear Fusion and Advanced Electromagnetic Technology Key Laboratory, Ministry of Education, and the School of Electrical and Electronics Engineering, Huazhong University of Science and Technology, Wuhan 430074, China (e-mail: luxinpei@hotmail.com).

Color versions of one or more of the figures in this paper are available online at http://ieeexplore.ieee.org.

Digital Object Identifier 10.1109/TPS.2009.2015321

Fig. 2. Photograph of the plasma. Applied voltage: 6 kV. Pulsewidth: 999.4 μs. Pulse repetition rate: 1 kHz. Ar flow rate: 200 sccm.

closed but not vacuum sealed. Therefore, when working gas is introduced from the left end of the quartz tube, the gas pressure inside the quartz tube stays close to the atmospheric pressure. There are always traces of air present in the discharge gap due to the diffusion of the ambient air. Working gases including He, Ar, and their mixtures with air can be used. The gas flow rate is controlled by a mass flow controller (MKS M100B). In this paper, Ar with a flow rate of 200 sccm is used. The two aluminum disks are connected to a pulsed power supply (amplitudes up to 10 kV, repetition rate up to 10 kHz, and pulsewidth variable from 200 ns to dc).

The applied voltages are measured by a P6015 Tektronix high-voltage probe and the currents by a CT1 Tektronix current probe. The voltage and current waveforms are recorded by a Tektronix DPO7104 broadband digital oscilloscope. The optical emission spectra are measured by a Princeton Instruments Acton SpectraHub 2500i spectrometer. A fast intensified charge-coupled device (ICCD) camera (Princeton Instruments, Model: PIMAX2, exposure time down to 0.5 ns) is used to capture the dynamics of the discharge.

III. Experimental Results

For all the experimental results reported in this paper, the applied voltage and the pulse repetition rate are fixed at 6 kV and 1 kHz, respectively. Ar is used as the working gas. The flow rate of Ar is fixed at 200 sccm.

When the Ar is introduced into the quartz tube and the pulsed dc voltages are applied to the two electrodes, a diffuse plasma can be generated inside the discharge gap. Fig. 2 shows the photograph of the plasma for a pulsewidth of 999.4 μs, pulse frequency of 1 kHz, and applied voltage of 6 kV.

It is noticed that there is no obvious visual change of the optical emission intensities when the pulsewidth increases from 600 ns to 999.4 μs. However, when the pulsewidth is further decreased to less than 600 ns or increased to more than 999.4 μs, the optical emission intensities are decreased significantly. To have a better understanding of this phenomenon, the I–V characteristics of the discharge have been investigated. Fig. 3(a)–(f) shows the I–V curves of the discharge under plasma-off (gap filled with air) and plasma-on (gap filled with Ar) conditions and for different pulsewidths. The $I_{\rm off}$ and $I_{\rm on}$ are the measured currents with the plasma off and on, respectively. $I_{\rm dis}$ is defined as the difference between the $I_{\rm off}$ and the $I_{\rm on}$. Because the capacitance of the gap during the discharge is unknown, it is difficult to calculate the actual discharge current from $I_{\rm dis}$. However, as we can see from Fig. 3(a), the displacement current is temporally separated from the discharge current, and it can therefore be separated by subtraction. On the secondary discharge, the displacement and the discharge currents are superimposed, which means that the voltage drop with the discharge on is not the same as the voltage drop at the gap without the discharge. The displacement current (without discharge) depends on the voltage drop at the gap. However, when the gap voltages are different for different conditions (plasma off and on), then the discharge current is not exactly the difference of the two currents. However, it is related to the discharge current. The similar I–V characteristics have been reported by Laroussi *et al.* [30]. For relatively short pulses, Fig. 3(a)–(c) shows the I–V curves of single pulses. For relatively long pulses, Fig. 3(d)–(f) shows the falling edge of the previous pulse and the rising edge of the consecutive pulse. For a pulsewidth of 200 ns, when the applied voltage starts to decrease, $I_{\rm dis}$ does not reach zero as can be seen in Fig. 3(a). $I_{\rm dis}$ drops to zero instantaneously because of the falling of the applied voltage. The negative current pulse corresponds to the secondary breakdown of the gap. This secondary discharge is ignited because of the voltage induced by the charges, which have accumulated on the surface of the quartz cap during the primary discharge [25]. With the increase of the pulsewidth, the first pulse of $I_{\rm dis}$ lasts longer. As the pulsewidth is increased to 600 ns [as shown in Fig. 3(b)], $I_{\rm dis}$ drops to zero before the falling of the applied voltage. Further increasing the pulsewidth to 2 and 998 μs has no obvious effect on $I_{\rm dis}$ as shown in Fig. 3(c) and (d); only the zero current duration is changed (i.e., the period with the applied voltage on but no discharge current). However, when the pulsewidth is increased to more than 999.4 μs, the primary discharge of the consecutive pulse starts to affect the secondary discharge at the falling edge of the previous voltage pulse, which can be seen from Fig. 3(e) and (f), respectively. When the pulsewidth is 999.8 μs, which corresponds to the voltage-off duration of 200 ns, the consecutive voltage pulse begins to rise before the $I_{\rm dis}$ of the previous pulse drops to zero. This is similar to the results in Fig. 3(a). However, there is one obvious difference between Fig. 3(a) and (f). For Fig. 3(a), because the voltage-on duration is too short, the primary discharge is affected by the secondary discharge produced by the same voltage pulse. On the other hand, for Fig. 3(f), because the voltage-off duration is too short, the secondary discharge generated by the previous voltage pulse is affected by the primary discharge of the consecutive voltage pulse.

The photograph of discharge (Fig. 2) shows that the plasma is uniform. To confirm that the plasma is actually diffuse, a high-speed ICCD camera is used to capture the temporal emission behavior of the plasma. Fig. 4 shows the high-speed

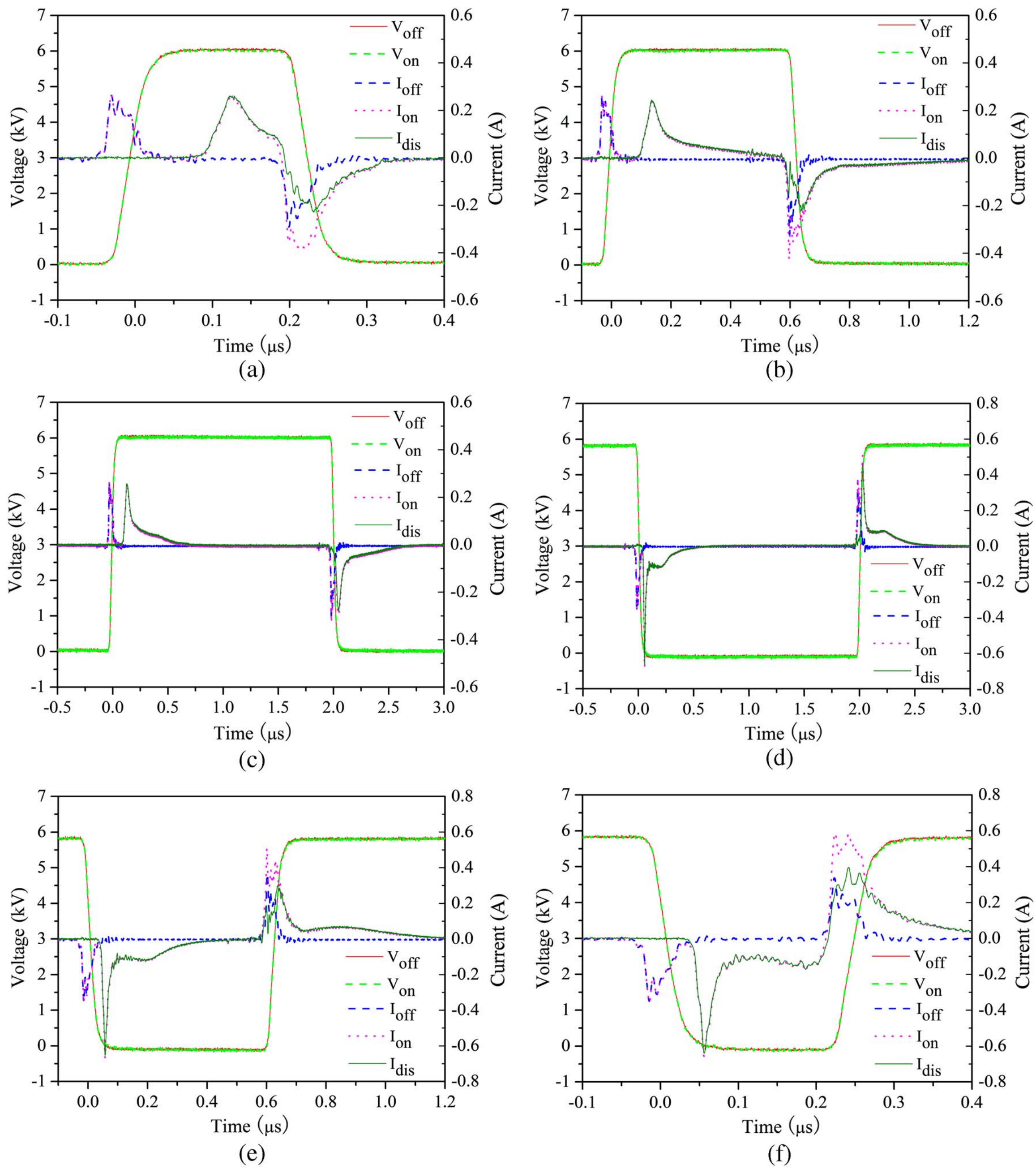

Fig. 3. Current–voltage characteristics of the discharge for different pulsewidths t_w. (a) $t_w = 200$ ns. (b) $t_w = 600$ ns. (c) $t_w = 2$ μs. (d) $t_w = 998$ μs. (e) $t_w = 999.4$ μs. (f) $t_w = 999.8$ μs. Pulse repetition rate is fixed at 1 kHz.

photographs of the plasma for the pulsewidth of 999.4 μs. The exposure time of the camera is 150 ns. Fig. 4(a) and (b) corresponds to the optical emission of the plasma from 0 to 150 ns and from 550 to 700 ns of Fig. 3(e), respectively. It should be emphasized that Fig. 4(a) corresponds to the secondary discharge ignited during the decaying period of the applied voltage. Thus, the electrode on the left serves as a cathode in this case. On the contrary, in Fig. 4(b), the electrode on the right serves as a cathode, which corresponds to the primary discharge generated during the rising period of the applied voltage. Both photographs clearly demonstrate that the discharge behaves like a diffused glowlike discharge, with a bright area near the cathode. Fig. 4(b) also shows the cathode glow, the Faraday dark space, the positive column, and the anode dark space (right to left). The high-speed photographs of the plasma for different pulsewidths are similar to those in Fig. 4. These discharges are also diffuse (not shown here).

To identify the various chemical species present in the discharge volume, optical emission spectroscopy (OES) is used. The OES allows the analysis of the optical emission of the atoms, ions, molecules, and radicals when they are excited by the electric field or by collisions with other particles. The wavelengths and intensities of the photons emitted are characteristic of the excited species. The gas temperature is important, and it can be determined by means of OES via the rotational temperature of nitrogen which is present in traces. Fig. 5 shows the emission spectra of the plasma in the range from 275 to 400 nm. Fig. 5 shows that the emission spectra are dominated

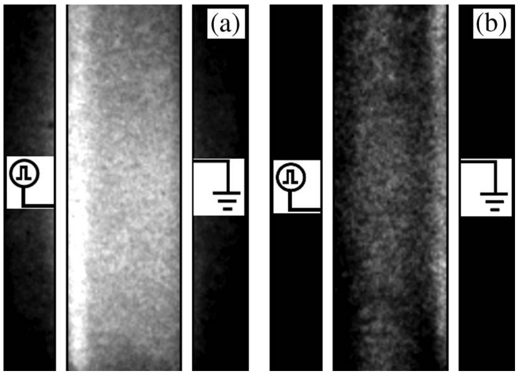

Fig. 4. High-speed photograph of the plasma. Exposure time: 150 ns. (a) 0–150 ns and (b) 550–700 ns. The times for (a) and (b) correspond to that in Fig. 3(e). The operation conditions are the same as in Fig. 2.

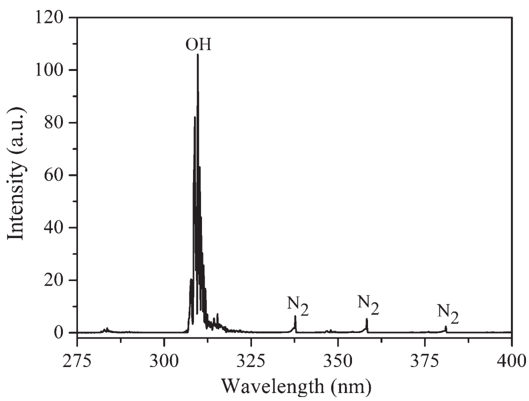

Fig. 5. Emission spectra of the plasma. The operation conditions are the same as in Fig. 2.

by OH and N_2 transitions. As aforementioned, the OH and N_2 emissions are due to the diffusion of the surrounding air. To determine the rotational and vibrational temperatures of the plasma, the emission spectra of the nitrogen second positive system are used. By comparing the simulated spectra of the $C^3\Pi_u - B^3\Pi_g(\Delta v = -2)$ band transition of nitrogen with the experimentally recorded spectra, the rotational and vibrational temperatures of the nitrogen can be obtained when the best fit is achieved [32]. The resolution of the spectroscopy is fixed at about 0.15 nm for these measurements. Fig. 6 shows the simulated and the experimental spectra of the plasma. It clearly shows that the simulated spectra at $T_{\mathrm{rot}} = 600$ K and $T_{\mathrm{vib}} =$ 1200 K fit well to the experimental spectra. The vibrational temperature T_{vib} of 1200 K is much higher than the rotational temperature T_{rot}. Because of the low energies needed for rotational excitation and the short transition times, molecules in the rotational states and the neutral gas molecules are in equilibrium. Therefore, the gas temperature is the same as the rotational temperature [32], [33].

The electron temperature of the plasma has not been measured. However, according to [31], the electron temperature of the plasma driven by the pulsed dc voltages can reach as high as 8 eV.

IV. Discussion

As we can see from Fig. 3(a)–(c), when the pulsewidth is shorter than 600 ns, the falling of the applied voltage starts

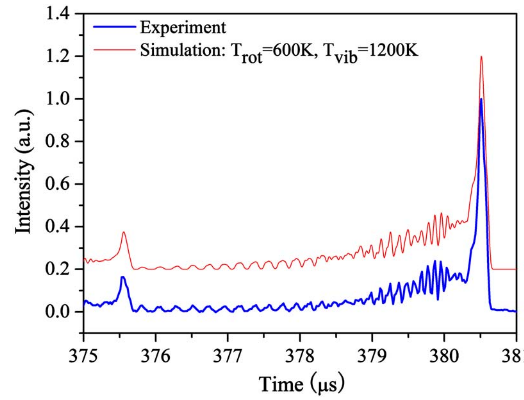

Fig. 6. Experimental and simulated emission spectra of the N_2 second positive system. The operation conditions are the same as in Fig. 2.

before I_{dis} drops to zero. Thus, the primary discharge is terminated because of the switching off of the applied voltage. Therefore, if a long primary discharge pulse is desired (e.g., for the generation of active species), then the pulsewidth of 600 ns or longer should be used. However, when the pulsewidth is longer than 999.4 μs, the rising of the consecutive voltage pulse appears before the secondary discharge generated by the previous voltage pulse is extinguished. Therefore, if a long secondary discharge is preferred, then the pulsewidth of 999.4 μs or shorter should be used.

It should be emphasized that the conclusions of this paper are applicable for DBDs. On the other hand, for barrier-free discharges, these conclusions cannot be applied. This is because of the possibility of glow-to-arc transitions when the pulsewidth is too long.

V. Conclusion

In conclusion, the effects of the pulsewidth on the DBDs were investigated. It was found that it is not necessary to have the pulsewidth as short as possible. High-speed photographs showed that diffuse Ar plasmas can be generated by pulsed dc voltages with pulsewidths varying from 0.2 μs to about 1 ms. However, when the pulsewidth is shorter than 600 ns or the break between the two consecutive pulses is shorter than 600 ns, the pulsewidths of the applied voltages affect the discharge current durations significantly. Therefore, if long primary and secondary discharge pulses are desired (e.g., for the generation of more active species), the pulsewidth should be longer than 600 ns but shorter than 999.4 μs for a pulse frequency of 1 kHz. Further study on the effect of the rising and falling times of the pulsed dc voltages are needed.

References

[1] R. Dorai and M. J. Kushner, "A model for plasma modification of polypropylene using atmospheric pressure discharges," *J. Phys. D, Appl. Phys.*, vol. 36, no. 6, pp. 666–685, Mar. 2003.

[2] P. Chu, "Plasma-treated biomaterials," *IEEE Trans. Plasma Sci.*, vol. 35, no. 2, pp. 181–187, Apr. 2007.

[3] M. Laroussi, "Low temperature plasma-based sterilization: Overview and state-of-the-art," *Plasma Process. Polym.*, vol. 2, no. 5, pp. 391–400, Jun. 2005.

[4] P. Bruggeman, L. Graham, J. Degroote, J. Vierendeels, and C. Leys, "Water surface deformation in strong electrical fields and its influence on electrical breakdown in a metal pin-water electrode system," *J. Phys. D, Appl. Phys.*, vol. 40, no. 16, pp. 4779–4786, Aug. 2007.

[5] G. Fridman, A. Brooks, M. Galasubramanian, A. Fridman, A. Gutsol, V. Vasilets, H. Ayan, and G. Friedman, "Comparison of direct and indirect effects of non-thermal atmospheric-pressure plasma on bacteria," *Plasma Process. Polym.*, vol. 4, no. 4, pp. 370–375, May 2007.

[6] E. Stoffels, I. Kieft, and R. Sladek, "Superficial treatment of mammalian cells using plasma needle," *J. Phys. D, Appl. Phys.*, vol. 36, no. 23, pp. 2908–2913, Dec. 2003.

[7] X. Lu, T. Ye, Y. Cao, Z. Sun, Q. Xiong, Z. Tang, Z. Xiong, J. Hu, Z. Jiang, and Y. Pan, "The roles of the various plasma agents in the inactivation of bacteria," *J. Appl. Phys.*, vol. 104, no. 5, p. 053 309, Sep. 2008.

[8] J. Goree, B. Liu, and D. Drake, "Gas flow dependence for plasma-needle disinfection of S-mutans bacteria," *J. Phys. D, Appl. Phys.*, vol. 39, no. 16, pp. 3479–3486, Aug. 2006.

[9] J. Kolb, A. Mohamed, R. Price, R. Swanson, A. Bowman, R. Chiavarini, M. Stacey, and K. Schoenbach, "Cold atmospheric pressure air plasma jet for medical applications," *Appl. Phys. Lett.*, vol. 92, no. 24, p. 241 501, Jun. 2008.

[10] R. Vidmar, "On the use of atmospheric-pressure plasmas as electromagnetic reflectors and absorbers," *IEEE Trans. Plasma Sci.*, vol. 18, no. 4, pp. 733–741, Aug. 1990.

[11] M. Laroussi, "Interaction of microwaves with atmospheric-pressure plasmas," *Int. J. Infrared Millim. Waves*, vol. 16, no. 12, pp. 2069–2083, Dec. 1995.

[12] K. Ostrikov, "Colloquium: Reactive plasmas as a versatile nanofabrication tool," *Rev. Mod. Phys.*, vol. 77, no. 2, pp. 489–511, Jun. 2005.

[13] K. Ostrikov and A. B. Murphy, "Plasma-aided nanofabrication: Where is the cutting edge?," *J. Phys. D, Appl. Phys.*, vol. 40, no. 8, pp. 2223–2241, Apr. 2007.

[14] K. H. Becker, U. Kogelschatz, and K. H. Schoenbach, *Non-Equilibrium Air Plasmas at Atmospheric Pressure*. London, U.K.: IOP Publ. Ltd., 2005.

[15] K. H. Becker, K. H. Schoenbach, and J. G. Eden, "Microplasmas and applications," *J. Phys. D, Appl. Phys.*, vol. 39, no. 3, pp. R55–R70, Feb. 2006.

[16] M. Laroussi and X. Lu, "Room-temperature atmospheric pressure plasma plume for biomedical applications," *Appl. Phys. Lett.*, vol. 87, no. 11, p. 113 902, Sep. 2005.

[17] D. Kim, J. Rhee, S. Moon, and W. Choe, "Study of geometrical and operational parameters controlling the micro jet atmospheric pressure plasma characteristics," *Appl. Phys. Lett.*, vol. 89, no. 6, p. 061 502, Aug. 2006.

[18] X. Lu, Z. Jiang, Q. Xiong, Z. Tang, X. Hu, and Y. Pan, "A single electrode room-temperature plasma jet device for biomedical applications," *Appl. Phys. Lett.*, vol. 92, no. 8, p. 081 502, Feb. 2008.

[19] D. Kim, J. Rhee, B. Gweon, S. Moon, and W. Choe, "Comparative study of atmospheric pressure low and radio frequency microjet plasmas produced in a single electrode configuration," *Appl. Phys. Lett.*, vol. 91, no. 15, p. 151 502, Oct. 2007.

[20] J. Goree, B. Liu, D. Drake, and E. Stoffels, "Killing of S. mutans bacteria using a plasma needle at atmospheric pressure," *IEEE Trans. Plasma Sci.*, vol. 34, no. 4, pp. 1317–1324, Aug. 2006.

[21] F. Leipold, R. H. Stark, A. El-Habachi, and K. H. Schoenbach, "Electron density measurements in an atmospheric pressure air plasma by means of infrared heterodyne interferometry," *J. Phys. D, Appl. Phys.*, vol. 33, no. 18, pp. 2268–2273, Sep. 2000.

[22] J. L. Walsh, J. J. Shi, and M. G. Kong, "Submicrosecond pulsed atmospheric glow discharges sustained without dielectric barriers at kilohertz frequencies," *Appl. Phys. Lett.*, vol. 89, no. 16, p. 161 505, Oct. 2006.

[23] X. Lu, Z. Jiang, Q. Xiong, Z. Tang, and Y. Pan, "A single electrode room-temperature plasma jet device for biomedical applications," *Appl. Phys. Lett.*, vol. 92, no. 15, p. 151 504, Apr. 2008.

[24] C. Jiang, A. A. Mohamed, R. H. Stark, J. H. Yuan, and K. H. Schoenbach, "Removal of volatile organic compounds in atmospheric pressure air by means of direct current glow discharges," *IEEE Trans. Plasma Sci.*, vol. 33, no. 2, pp. 1416–1425, Aug. 2005.

[25] X. Lu and M. Laroussi, "Dynamics of an atmospheric pressure plasma plume generated by submicrosecond voltage pulses," *J. Appl. Phys.*, vol. 100, no. 6, p. 063 302, Sep. 2006.

[26] T. Shao, P. Yan, K. Long, and S. Zhang, "Dielectric-barrier discharge excitated by repetitive nanosecond pulses in air at atmospheric pressure," *IEEE Trans. Plasma Sci.*, vol. 36, no. 4, pp. 1358–1359, Aug. 2008.

[27] A. Kirpichnikov and A. Starikovskii, "Nanosecond pulsed discharge—Always uniform?" *IEEE Trans. Plasma Sci.*, vol. 36, no. 4, pp. 898–899, Aug. 2008.

[28] R. P. Mildren, R. J. Carman, and I. S. Falconer, "Visible and VUV images of dielectric barrier discharges in Xe," *J. Phys. D, Appl. Phys.*, vol. 34, no. 23, pp. 3378–3382, Nov. 2001.

[29] S. Liu and M. Neiger, "Excitation of dielectric barrier discharges by unipolar submicrosecond square pulses," *J. Phys. D, Appl. Phys.*, vol. 34, pp. 1632–1638, Jun. 2001.

[30] M. Laroussi, X. Lu, V. Kolobov, and R. Arslanbekov, "Power consideration in the pulsed dielectric barrier discharge at atmospheric pressure," *J. Appl. Phys.*, vol. 96, no. 5, pp. 3028–3030, Jun. 2004.

[31] X. Lu and M. Laroussi, "Electron density and temperature measurement of an atmospheric pressure plasma by millimeter wave interferometer," *Appl. Phys. Lett.*, vol. 92, no. 9, p. 051 501, Feb. 2008.

[32] G. Faure and S. M. Shkol'nik, "Determination of rotational and vibrational temperatures in a discharge with liquid non-metallic electrodes in air at atmospheric pressure," *J. Phys. D, Appl. Phys.*, vol. 31, no. 10, pp. 1212–1218, May 1998.

[33] G. Herzberg, "Molecular spectra and molecular structure I," in *Spectra of Diatomic Molecules*. Princeton, NJ: Van Nostrand, 1953.

XinPei Lu (M'06–SM'07) received the Ph.D. degree in electrical engineering from Huazhong University of Science and Technology, Wuhan, China, in 2001.

From 2002 to 2006, he was with the Applied Plasma Technology Laboratory, Old Dominion University, as a Research Associate. Since 2007, he has been with Huazhong University of Science and Technology, where he is currently a Professor (Chang Jiang Scholar) with the School of Electrical and Electronics Engineering and where he is also with the Nuclear Fusion and Advanced Electromagnetic Technology Key Laboratory, Ministry of Education. His research interests include low-temperature plasma sources and their applications, modeling of low-temperature plasmas, plasma diagnostics, and pulse power technology. He is the author or coauthor of about 50 scientific articles in these areas.

Dr. Lu served as a Guest Editor of the IEEE TRANSACTIONS ON PLASMA SCIENCE and as Session Chair at the International Conference on Plasma Science for several years.

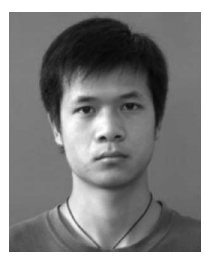

Qing Xiong received the B.E degree in electrical engineering from Southwest Jiaotong University, Chengdu, China, in 2007. He is currently working toward the Ph.D. degree with the Nuclear Fusion and Advanced Electromagnetic Technology Key Laboratory, Ministry of Education, and the School of Electrical and Electronics Engineering, Huazhong University of Science and Technology, Wuhan, China.

His research interests are focused on the diagnostics and applications of atmospheric-pressure nonequilibrium plasma sources.

ZiLan Xiong received the B.E degree in electrical engineering in 2008 from the Huazhong University of Science and Technology, Wuhan, China, where she is currently working toward the M.S. degree with the Nuclear Fusion and Advanced Electromagnetic Technology Key Laboratory, Ministry of Education, and the School of Electrical and Electronics Engineering.

She is devoted to the study of plasma medicine and the applications of atmospheric-pressure nonequilibrium plasma sources.

YuBin Xian received the B.S. degree in 2007 from the Huazhong University of Science and Technology, Wuhan, China, where he is currently working toward the M.S. degree with the Nuclear Fusion and Advanced Electromagnetic Technology Key Laboratory, Ministry of Education, and the School of Electrical and Electronics Engineering.

His research interests include plasma medicine and the applications of atmospheric-pressure nonequilibrium plasma sources.

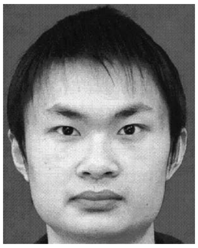

Fei Zhou received the B.S. degree in 2007 from the Huazhong University of Science and Technology, Wuhan, China, where he is currently working toward the M.S. degree with the Nuclear Fusion and Advanced Electromagnetic Technology Key Laboratory, Ministry of Education, and the School of Electrical and Electronics Engineering.

His research interests include plasma medicine and the applications of atmospheric-pressure nonequilibrium plasma sources.

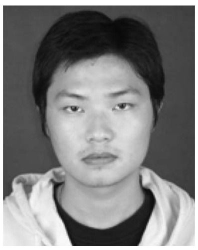

Jing Hu received the B.E degree in electrical engineering in 2008 from the Huazhong University of Science and Technology, Wuhan, China, where he is currently working toward the M.S. degree with the Nuclear Fusion and Advanced Electromagnetic Technology Key Laboratory, Ministry of Education, and the School of Electrical and Electronics Engineering.

He is devoted to the study of plasma medicine and the applications of atmospheric-pressure nonequilibrium plasma sources.

WeiWei Gong received the B.M. degree in clinical medicine in 2008 from the Huazhong University of Science and Technology, Wuhan, China, where he is currently working toward the M.S. degree with the the Nuclear Fusion and Advanced Electromagnetic Technology Key Laboratory, Ministry of Education, and the School of Electrical and Electronics Engineering.

His research interests include plasma medicine and the applications of atmospheric-pressure nonequilibrium plasma sources.

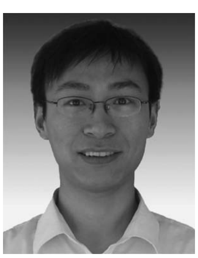

ChangLin Zhou received the M.S. degree in physics from Anhui University, Hefei, China, in 2008. He is currently working toward the Ph.D. degree with the Nuclear Fusion and Advanced Electromagnetic Technology Key Laboratory, Ministry of Education, and the School of Electrical and Electronics Engineering, Huazhong University of Science and Technology, Wuhan, China.

His research interests include plasma medicine and the applications of atmospheric-pressure nonequilibrium plasma sources.

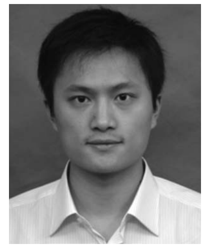

ZhiYuan Tang received the B.E. degree in electrical engineering from Hunan University, Changsha, China, in 2007. He is currently working toward the M.S. degree with the Nuclear Fusion and Advanced Electromagnetic Technology Key Laboratory, Ministry of Education, and the School of Electrical and Electronics Engineering, Huazhong University of Science and Technology, Wuhan, China.

His research interests include plasma medicine and the applications of atmospheric-pressure nonequilibrium plasma sources.

ZhongHe Jiang received the M.S. degree in particle and nucleus physics from the Institute of Modern Physics, Chinese Academy of Science, Lanzhou, China, in 2000 and the Ph.D. degree from Huazhong University of Science and Technology, Wuhan, China, in 2004.

Since 2004, he has been a Researcher with the School of Electrical and Electronics Engineering, Huazhong University of Science and Technology, where he is also with the Nuclear Fusion and Advanced Electromagnetic Technology Key Laboratory, Ministry of Education. His research interests include the simulation of atmospheric plasma and the simulation of the interaction between electromagnetic wave and plasma.

Yuan Pan received the B.S. degree in electrical engineering from Huazhong University of Science and Technology, Wuhan, China, in 1955.

Then, he was with the Institute of 401, the Institute of 585, the Institute of Plasma Physics, CAS, the Joint European Tokamak, and the Fusion Research Center, University of Texas. Currently, he is a Professor and the Honorary Dean of the School of Electrical and Electronics Engineering, Huazhong University of Science and Technology, where he is also with the Nuclear Fusion and Advanced Electromagnetic Technology Key Laboratory, Ministry of Education. His main research interests include magnetic confinement nuclear fusion, high power pulse source technology, superconducting electric power, and pulse power technology. He is the author or coauthor of about 100 scientific articles in these areas.

Dr. Pan is a member of the Chinese committee of experts of the international thermonuclear experimental reactor. He was elected as a member of the Chinese Academy of Engineering.